

Universal quantum computation via scalable measurement-free error correction

Stefano Veroni,¹ Alexandru Paler,^{1,2} and Giacomo Giudice^{1,*}

¹*PlanQC GmbH, Münchener Str. 34, 85748 Garching, Germany*

²*Aalto University, 02150 Espoo, Finland*

(Dated: January 17, 2025)

We show that universal quantum computation can be made fault-tolerant without intermediate measurements. To this end, we introduce a measurement-free deformation protocol of the Bacon-Shor code to realize a logical CCZ gate, enabling a universal set of fault-tolerant operations. Independently, we demonstrate that certain stabilizer codes can be concatenated in a measurement-free way without having to rely on a universal logical gate set. This is achieved by means of the disposable Toffoli gadget, which realizes the feedback operation in a resource-efficient way. For the purpose of benchmarking the proposed protocols with circuit-level noise, we implement an efficient method to simulate non-Clifford circuits consisting of few Hadamard gates. In particular, our findings support that below-breakeven logical performance is achievable with a depolarizing error rate below 10^{-3} . Altogether, the deformation protocol and the Toffoli gadget provide a blueprint for a fully fault-tolerant architecture without any feed-forward operation, which is particularly suited for state-of-the-art neutral-atom platforms.

I. INTRODUCTION

Large-scale quantum computation will rely on the implementation of *quantum error correction* (QEC), which is essential for accurate quantum information processing [1, 2]. Given the inherently noisy nature of quantum hardware, it is crucial to engineer systems that can mitigate the spread of faults. The strategy involves encoding logical information into a specific subspace within the broader physical Hilbert space—often through non-local encoding—allowing the system to be resilient against local errors. This redundancy, while effective, significantly increases the resource demands of QEC. As a result, the optimal choice of error-correction protocol should be tailored to the specific quantum computing hardware, both to minimize overhead and exploit the platform’s unique characteristics. Despite these complexities, recent experimental breakthroughs have marked remarkable progress in QEC across different architectures, such as superconducting qubits [3–11], trapped ions [12–21], nitrogen vacancies in diamonds [22], and neutral-atom arrays [23–26].

In traditional QEC approaches, a partial measurement of the system, known as the *error syndrome*, is used to inform a classical decoding algorithm, which then determines the corrective actions applied to the system—either through physical intervention or software-based adjustments [1]. These partial measurements often correspond to *stabilizer* operators, which commute with logical operators, such that the logical state remains unaffected [27].

In some quantum computing platforms, such as those based on neutral atoms or trapped ions, the relatively slow nature of such measurements often hinders the efficiency of this syndrome extraction [17, 18, 23, 28–32]. An alternative approach, *measurement-free* (MF) QEC, has emerged as a promising solution [33–39], replacing classical processing with purely unitary dynamics. In MF QEC,

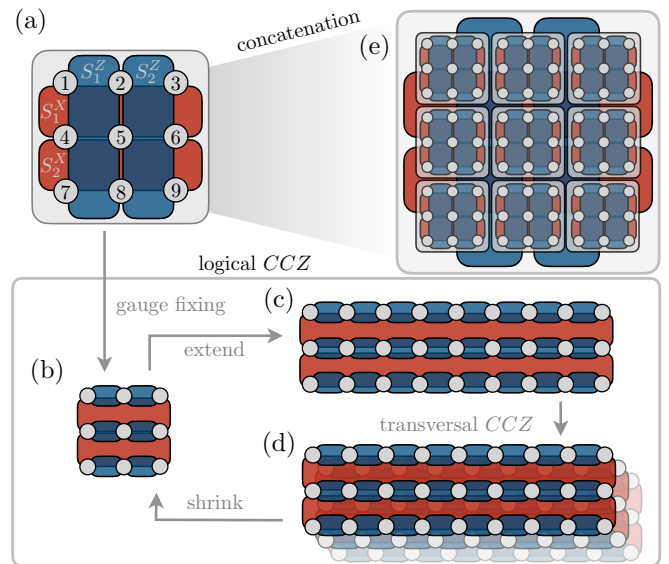


Figure 1. (a) The stabilizers of the 3×3 Bacon-Shor code, with red (blue) areas depicting the support of X -type (Z -type) stabilizer operators. (b) Any Bacon-Shor code has a gauge freedom. In particular, the pairwise $Z_i Z_j$ gauges along rows can be chosen to be $+1$, resulting in a Shor code. We call this the *Shor gauge*. To perform a logical CCZ , each logical qubit must start from this gauge, and then be extended to a 3×9 Bacon-Shor code, as shown in (c). The logical CCZ is then performed between logical qubits, by a transversal application of physical CCZ gates, with permutations across the columns. (d) To return to the original 3×3 configuration, a shrink move is performed. (e) To increase the tolerance to errors, *concatenation* of the same code is performed, where the data qubits of a code are composed of logical qubits at a lower level.

the dissipative dynamics needed to remove the entropy introduced by noise is achieved through reset operations or a continuous supply of fresh ancilla qubits, which has been recently demonstrated in neutral-atom platforms [40–42]. In particular, the first fully *fault-tolerant* (FT) pro-

* giacomo.giudice@planqc.eu

posal correcting a single error was achieved in Ref. [38], by adapting Steane-type error correction techniques [43]. Later, some of the authors of this work showed that by using redundant syndrome information, low-overhead alternatives can be formulated as well [39].

The notion of fault-tolerance is essential for the design of an error-corrected quantum computer. Broadly speaking, an FT implementation is capable of limiting error propagation, thus reducing the logical error rates, as long as the physical error rate remains below a certain threshold. This is relevant both for the QEC round (which must not inject additional errors during its noisy execution), and for logical operations. *Transversal* operations are particularly appealing, since they are straightforwardly FT [1]. Transversal operations correspond to a single-layer of physical gates, each of which acts on at most one physical qubit of each logical qubit. Therefore, errors can propagate between logical qubits, but remain correctable, since QEC is applied to each logical qubit individually.

However, it is well known that no QEC code can have a transversal universal gate set [44], and, in particular, the only transversal gates for two-dimensional codes are unitaries belonging to the Clifford group [45]. Several ways have been proposed to get around these no-go results. These include magic state distillation [46–50], code switching between appropriate codes [51–53], using non-local connectivity between Bacon-Shor codes [54], implementing pieceable constructions where operations are intertwined with intermediate error correction [55], or allowing for a loss of distance in concatenated codes [56–58].

The main theoretical challenges for MF QEC are two-fold: (*i*) implementing universal quantum computation at the logical level, and (*ii*) demonstrating scalability beyond small-distance codes. During the completion of this work, the authors of Ref. [59] demonstrated MF code-switching between color-codes to implement a universal set of logical gates. Equipped with this universal set, it is then possible to concatenate the code with itself to reach higher distances.

We tackle the aforementioned challenges with a different approach. We show that (*i*) a *universal gate set* is achievable with the Bacon-Shor code, by exploiting transversal operations and a MF code deformation procedure to realize a transversal *CCZ* gate; and (*ii*) a universal gate set is *not required* to concatenate MF QEC, but that it can be scaled up efficiently.

This work is organized as follows. In Sec. II, we review the Bacon-Shor code, which was shown to yield the best performance among currently devised MF schemes [37–39]. In Sec. III, we construct a MF procedure to *deform* the code and exploit the protocol proposed in Ref. [54] to implement a logical *CCZ* gate, thus enabling MF universal quantum computation. We then turn to address the second challenge in Sec. IV. While this code deformation allows for a universal logical gates set, we take a different approach and implement MF QEC on concatenated codes *without* the need for a universal gate set. Inspired by Ref. [33], we implement a feedback opera-

tion which we dub the *disposable Toffoli gadget* and is significantly more efficient than using the aforementioned logical *CCZ* construction. The essence of this gadget is to *unencode* ancilla qubits—storing stabilizer information—into a repetition code and then exploiting the (partial) transversality between repetition codes and a target code from the Calderbank-Steane-Shor (CSS) [60, 61] family. Finally, in Sec. V we discuss potential advantages of this measurement-free approach, and how they are particularly suitable for neutral-atom platforms.

II. THE BACON-SHOR CODE

In this section, we introduce the Bacon-Shor code (Sec. II A), we summarize the construction for logical *CCZ* used in Ref. [54] (Sec. II B), and introduce some properties relating the Bacon-Shor code and the repetition code (Sec. II C), which we will use throughout this paper.

A. Notation

The main properties of a QEC code are typically described by the triplet $\llbracket n, k, d \rrbracket$, where n is the number of physical qubits, k is the number of logical qubits, and d is the code distance, i.e. the minimum number of single-qubit operations required to get from one codeword to another. Additionally, we define t as the number of *tolerable* errors—i.e. all errors of weight smaller or equal than t can be corrected—satisfying $t \leq \lfloor \frac{d-1}{2} \rfloor$.

In this work, we will be focusing on the Bacon-Shor code [62, 63]. This code essentially combines a n_1 -qubit repetition code against Z errors with a n_2 -qubit repetition code against X errors in a $n_1 \times n_2$ array of data qubits. Labeling the qubits in this array with (i, j) , the stabilizers for the $\llbracket n_1 n_2, 1, \min(n_1, n_2) \rrbracket$ Bacon-Shor code are generated from

$$S_i^X = \prod_{j=1}^{n_2} X_{i,j} X_{i+1,j}, \quad S_i^Z = \prod_{i=1}^{n_1} Z_{i,j} Z_{i,j+1}. \quad (1)$$

These are depicted in Fig. 1(a) for the minimal error-correcting instance $\llbracket 9, 1, 3 \rrbracket$. This specific instance is the main focus of this paper, as its MF QEC implementation, proposed in Ref. [39], is particularly simple.

The logical operators are $X_L = \prod_j X_{i,j}$ and $Z_L = \prod_i Z_{i,j}$ for any value of i or j respectively, as shown in Fig. 2(a). As with all CSS codes, all logical Pauli operations are trivially transversal. Additionally, the logical CNOT can be implemented transversally, by performing a CNOT between pairs of data qubits. Additionally, the logical Hadamard gate is also transversal—it corresponds to a Hadamard gate on all data qubits and a relabeling of the physical qubits, which can be achieved with a reflection along the diagonal to swap X and Z stabilizers [63].

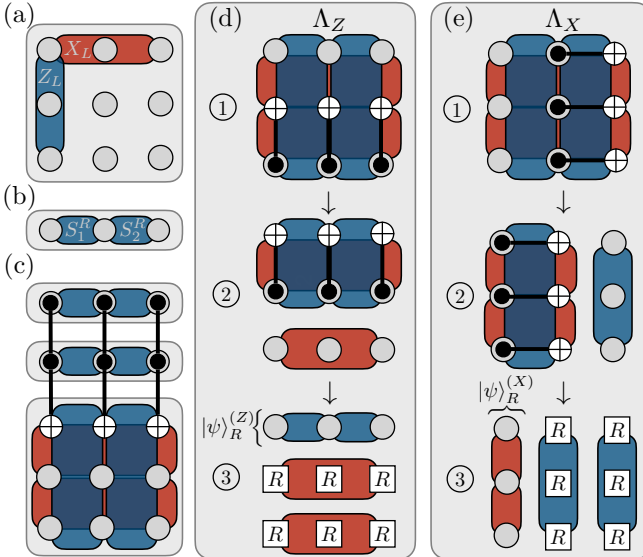


Figure 2. (a) The logical operators of a Bacon-Shor code correspond to a single row (X_L) or column (Z_L). (b) A bit-flip repetition code is formed by pairwise $S_i^R = Z_i Z_{i+1}$ stabilizers along a chain. (c) A transversal CCX between a three-qubit repetition code and $d = 3$ Bacon-Shor code. Note that this gate is only unidirectional. (d)–(e) The unencoding operation Λ_Z (Λ_X) maps a Bacon-Shor code down to a bit-flip (phase-flip) repetition code. Intuitively, each column (row), supporting a separate representation of the relevant logical operator, is mapped to a qubit of the resulting repetition code. The stabilizers after each layer of gates are depicted.

The Bacon-Shor code is a subsystem code [1, 62], such that multiple states encode the same logical codeword. These states are equivalent up to multiplication and/or measurement of *gauge operators*, which commute with the stabilizers and logical operators, thus not affecting the logical information. The gauge group is generated by the pairs $X_{i,j}X_{i+1,j}$ ($Z_{i,j}Z_{i,j+1}$) acting on qubits in the same column (row). In what follows, we will be mainly interested in the ‘Shor gauge’ of the code, where all $Z_{i,j}Z_{i,j+1}$ gauge operators have eigenvalue +1. In this gauge, the codewords are equivalent to those of Shor’s code [64]. In particular, in this gauge certain logical states become a tensor product of cat states

$$|\pm\rangle_L^{(Z)} = \frac{1}{2\sqrt{2}} (|000\rangle \pm |111\rangle)^{\otimes 3}. \quad (2)$$

These states are particularly important, since they can be prepared fault-tolerantly without additional overhead [12]. We will denote the opposite gauge, in which all $X_{i,j}X_{i+1,j}$ have eigenvalue +1, as the ‘anti-Shor’ gauge. In this gauge, the state $|0\rangle_L$ and $|1\rangle_L$ have a similar structure Eq. (2), this time as a tensor product of cat states along the columns instead of rows. A mixed gauge can be chosen as well, as long as the gauge operators commute. In particular, the rotated surface is a specific gauge choice of the Bacon-Shor code [65].

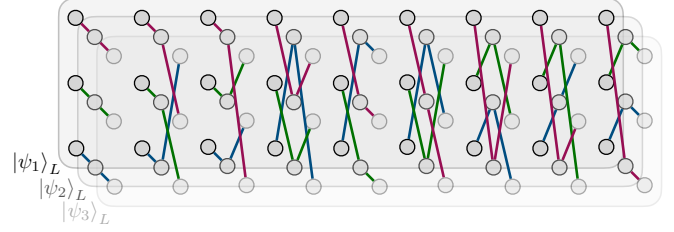


Figure 3. Graphical depiction of the connectivity required for the transversal $CCZ_L |\psi_1\psi_2\psi_3\rangle_L$ between three logical states $|\psi_k\rangle_L$, $k = 1, 2, 3$, each encoded in the 3×9 the Bacon-Shor codes, in the Shor gauge. Different colors correspond to different CCZ gates between rows, and highlight that the permutations occur only across columns.

B. Logical CCZ

It was shown in Ref. [54] that a $m \times m^k$ Bacon-Shor code in the Shor gauge supports a transversal logical $C^k Z_L$ —at the price of losing the transversal logical Hadamard. In particular, as shown in Fig. 3, the logical CCZ_L between three 3×9 logical qubits is implemented by a *single layer* of 27 physical CCZ gates

$$CCZ_L = \prod_{j=0}^8 \prod_{i=0}^2 CCZ_{(i,j), (i \oplus [j/3], j), (i \oplus j, j)}, \quad (3)$$

where it is assumed that (i, j) indices start from 0 for ease of notation, and \oplus represents addition modulo 3.

As the Hadamard and CCZ gates together define a universal gate set, it is then sufficient to demonstrate that these two gates can be performed fault-tolerantly. As our starting point, we choose the 3×3 Bacon-Shor code, since it has a MF QEC implementation [39], as well as a straightforward transversal Hadamard gate. In Sec. III, we will demonstrate a fully MF protocol to implement a logical CCZ : first, the code is mapped to the Shor gauge, by means of a *gauge fixing* procedure (Fig. 1(b)), then extended to a 3×9 code (Fig. 1(c)); now the logical CCZ can be performed using Eq. (3), cf. Fig. 1(d). To return to the original code, we then shrink it down to a 3×3 code (Fig. 1(b)).

C. Relationship with the repetition code

Before continuing with the logical protocol, we wish to flesh out some properties connecting CSS codes with repetition codes, which we will exploit later on. The bit-flip (phase-flip) repetition code is defined on n qubits by pairwise stabilizers $S_i^R = Z_i Z_{i+1}$ ($S_i^R = X_i X_{i+1}$), cf. Fig. 2(b), and protects against X -type (Z -type) errors. The respective logical codewords are $|0/1\rangle_R^{(Z)} = |0/1\rangle^{\otimes n}$ and $|\pm\rangle_R^{(X)} = |\pm\rangle^{\otimes n}$. Generalizing the constructions proposed in Ref. [33], throughout this work we exploit the fact that *unidirectional* transversal gates exist between

repetition codes and CSS codes. In particular, a logical $C^k X$ ($C^k Z$) gate on a distance- d code can be controlled from k length- d bit-flip repetition codes, as illustrated in Fig. 2(c) for the Toffoli gate. This gate is transversal, as it is composed of d physical $C^k X$ ($C^k Z$) gates targeting d qubits supporting the X_L (Z_L) operator of the code. As explained in App. A, the stabilizer structure is preserved.

Additionally, we introduce a gadget to convert a logical codeword to a codeword of the repetition code. We call this an *unencoding* gadget, and can be used when partial protection against either bit flips or phase flips is sufficient. For an arbitrary logical state $|\psi\rangle_L = \alpha|0\rangle_L + \beta|1\rangle_L$, $|\alpha|^2 + |\beta|^2 = 1$, we introduce the unencoding operations

$$\Lambda_{X/Z} |\psi\rangle_L = |\psi\rangle_R^{(X/Z)} \otimes |0\rangle^{\otimes 6}, \quad (4)$$

which converts it to $|\psi\rangle_R^{(X/Z)} = \alpha|0\rangle_R^{(X/Z)} + \beta|1\rangle_R^{(X/Z)}$. Notice that these gadgets are not unitary, since information about the gauge choice is removed by the reset operations R . The implementation of the unencoding gadgets for the 3×3 Bacon-Shor code is illustrated in Figs. 2(d) and 2(e), and is similar to the reverse of the encoding circuit. Effectively, the unencoding gadget Λ_Z (Λ_X) maps the value of each column's Z_L (row's X_L) on a qubit of the resulting repetition code—thus it is applicable to any gauge choice of the Bacon-Shor code, e.g. the rotated surface code. For generic codes, such gadgets can be implemented, albeit with a larger overhead, by repeatedly performing Hadamard tests on different logical strings of the logical operators, and performing a majority vote, as was proposed in Ref. [33].

III. MEASUREMENT-FREE FAULT-TOLERANT LOGICAL CCZ

In this section, we discuss in detail the protocol for a fault-tolerant CCZ_L , schematically illustrated in Fig. 1. For the distance-3 Bacon-Shor code, this corresponds to the protocol in Fig. 4. We describe in more detail this protocol in Sec. IIIA and benchmark it under depolarizing noise in Sec. IIIB.

A. Circuit design

To apply Eq. (3), the Shor gauge must be first enforced on the code. In general, this is necessary in a FT quantum computation even if we initialized logical states in the correct gauge, since the H gate exchanges the Shor and anti-Shor gauge. Furthermore, the QEC circuit proposed in Ref. [39], and later adapted in Sec. IV, corrects every single-qubit error up to a gauge operator. From a measurement-free perspective, fixing the gauge is somewhat more challenging than correcting single errors, as we must account for both gauge flips as well as possible single-qubit errors, so the heuristics developed in Ref. [39] are not applicable. To gauge a logical state, we propose

two different alternatives: (i) a *teleportation* protocol and (ii) *Steane-type gauge fixing*. Both have similar performances under depolarizing noise, so we focus on the former, while the latter is relegated to App. B.

In the teleportation protocol, the logical state is moved to a fresh register, which is initialized in the correct gauge. The gauge information of the original state is removed by the unencoding gadget. Its MF variant is illustrated in Fig. 4(b), and requires two additional logical registers. Note that it can also correct single bit-flip errors, and has the added benefit of converting potential leakage errors into computational errors.

To extend a Bacon-Shor code in the Shor gauge from 3×3 to 3×9 , it is sufficient to perform two consecutive transversal CNOTs from the code to a $|0\rangle^{\otimes 9}$, cf. Fig. 4(c). However, this may propagate bit flips that may lead to uncorrectable errors, so to make the procedure FT we introduce bit-flip corrections $C_X^{(R)}$ along the rows, cf. Fig. 4(d). To shrink back a logical state to the 3×3 code, it is then sufficient to perform a series of CNOTs, illustrated in Fig. 4(e). Since the circuits act independently on each row, phase-flips cannot propagate to different rows and remain correctable. In principle, such schemes can be generalized to any 3×3^k Bacon-Shor code, to directly perform transversal $C^k Z$ gates [54].

B. Numerical results

We benchmark the scheme in Fig. 4 against the hardware-agnostic depolarizing noise, where after each gate, a random Pauli error is applied with probability p . That is, given the set of Pauli strings of length ℓ , i.e., $\mathcal{P}_\ell = \{I, X, Y, Z\}^{\otimes \ell}$, any ℓ -qubit gate is followed by the channel

$$\mathcal{E}(\rho) = (1-p)\rho + \frac{p}{|\mathcal{P}_\ell| - 1} \sum_{\substack{P \in \mathcal{P}_\ell \\ P \neq I^{\otimes \ell}}} P \rho P^\dagger. \quad (5)$$

Considering that the circuits contain more than 80 qubits and 27 physical CCZ gates, both state vector simulators as well as Clifford simulators are not suitable. Nevertheless, the logical states contain very few non-zero amplitudes in the computational basis (up to 128 for $|\pm\rangle_L$ in the anti-Shor gauge), so the state vector is extremely *sparse*. If one simply keeps track of these non-zero entries—much as one would do with “pen and paper” calculation—the simulations can be performed with very moderate computational resources.

For this task, we develop `SparseStates.jl` [66] a simulation package in Julia which can efficiently simulate circuits with few *branching* gates, i.e. gates that create superpositions in the computational basis (which are only H gates in our case). This allows us to compute thousands of circuit samples per second with circuits involving more than 100 qubits and hundreds of Toffoli-like gates. To the best of our knowledge, only Ref. [67] implements a similar method, based on hash maps, and with further gate

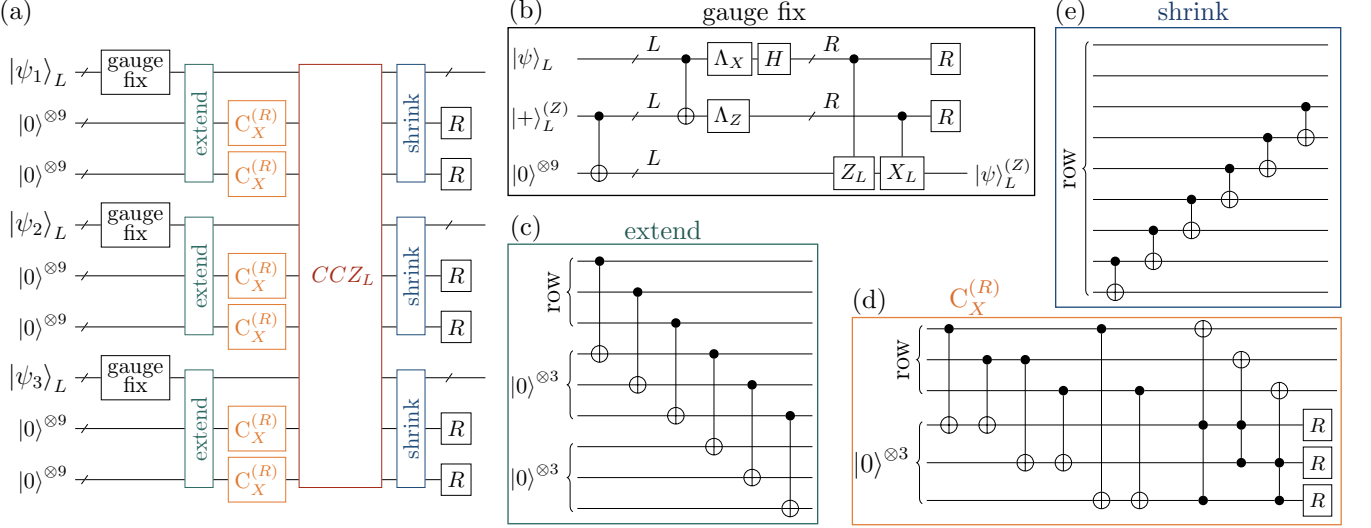


Figure 4. (a) Components of the protocol for the CCZ_L gate between 3×3 Bacon-Shor codes. (b) Measurent-free gauge fixing by teleportation. A logical Bell state $(|00\rangle_L + |11\rangle_L)/\sqrt{2}$ is first prepared in the Shor gauge. Note that, because the $|+\rangle_L$ is prepared in the Shor gauge, the last logical qubit does not need to be prepared in $|0\rangle_L$. This auxiliary state is then entangled with the logical state, and then MF teleportation using CX and CZ gates is performed, by first unencoding to the repetition code, cf. Sec. II C. (c) The extend gadget deforms a 3×3 Bacon-Shor code to its 3×9 variant, by exploiting the Shor gauge in the previous step. (d) A measurement-free error-correction round for the repetition code, used to correct for single bit flips on each triplet of each row of the logical states. (e) The extend gadget is reversed by a shrink gadget, bringing the logical state back to a 3×3 Bacon-Shor code.

rearrangements for the optimized simulation of quantum algorithms. Instead, our state-vector implementation is array based, which allows us to perform most operations in place—avoid unnecessary memory allocations—and opening up the possibility to exploit vectorized instructions available on most general-purpose processors.

By starting from the ideal codewords $|111\rangle_L$ and $|+++ \rangle_L$, we sample different Kraus operators according to Eq. (5), simulating up to 2^{24} realization or 2^{10} failures, whichever comes first. To compute the average logical fidelity F_{CCZ} up to the degeneracy of the gauge choice, we expand the overlap with the target state $|\phi\rangle_L$ as a sum over expectation values of logical Pauli strings on the logical support

$$F_{CCZ} = |\langle \psi | \phi \rangle_L|^2 = \sum_{P_L \in \mathcal{P}} c_{P_L} \langle \psi | P_L | \psi \rangle_L, \quad (6)$$

where $c_{P_L} = \langle \phi | P_L | \phi \rangle_L$.

In Fig. 5, the results are shown for the different initial states. The quadratic scaling law of the logical error confirms the fault-tolerance of the scheme. Overall, there is an order of magnitude difference for the two initial states $|+++ \rangle_L$, which creates a multipartite entangled state, and $|111\rangle_L$, which is just mapped to itself. The initial gauge of the code, instead, does not impact the logical performance of the scheme (see also App. B).

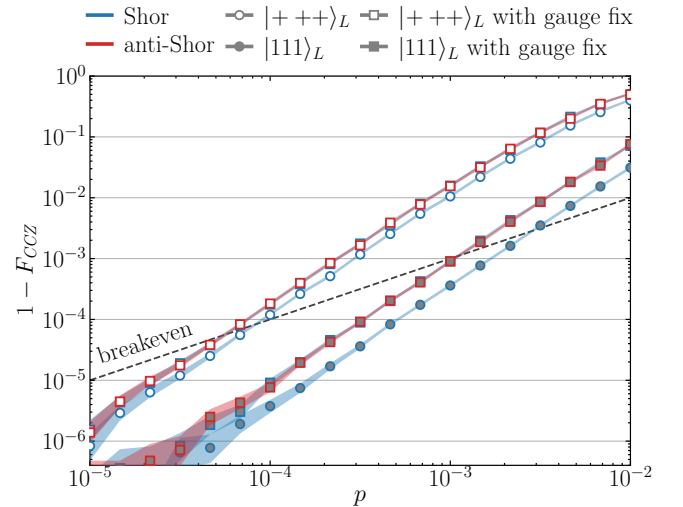


Figure 5. Error rate of the logical CCZ gate under depolarizing noise, computed using Eq. (6). The performance is benchmarked for input $|+++ \rangle_L$ (white-filled) and $|111\rangle_L$ (grey-filled) states, starting in the Shor (blue) or anti-Shor (red) gauges, and encoded without errors. Without gauge fixing, only starting from the Shor gauge is fault-tolerant. Shaded regions correspond to 95 % confidence intervals.

IV. MEASUREMENT-FREE CONCATENATION

Having demonstrated all the ingredients for FT and MF universal computation, in this section we show that the Bacon-Shor code can be scaled up by means of concatena-

tion, thus achieving exponential suppression of noise. In subsection IV A we introduce code concatenation and how it applies to MF QEC. Then, in Sec. IV B we present an optimized QEC protocol for the concatenated Bacon-Shor code. Using the disposable Toffoli gadget, we engineer an efficient feedback in the case where the information of the controlling qubits needs not be protected nor preserved, such as for ancilla qubits. We therefore do not have to use the code deformation procedure developed in Sec. III. Numerical benchmark are presented in Sec. IV C.

A. Code concatenation

We explore repeated *concatenation* of the same code, which we denote as

$$\mathcal{C}_N = \underbrace{\mathcal{C} \circ \cdots \circ \mathcal{C}}_{N \text{ times}}, \quad (7)$$

such that the first layer of concatenation is $\mathcal{C}_1 \equiv \mathcal{C}$. The concatenation operation \circ is a way of combining two codes: the logical qubits of the *inner* code are used as physical qubits of the *outer* one, cf. Fig. 1(e). By recursively applying this operation, we can then construct a N -layer concatenated code.

Concatenation is a modular way of increasing the code distance. Indeed, by concatenating N times a CSS code of distance d , we obtain $d_N = d^N$. The number of errors t_N that we can correct depends on the decoding strategy. Since in MF QEC decoding and corrections are operated by noisy quantum circuits rather than via classical processing, the complexity of the available feedback operations is in practice limited. In the simplest decoding strategy each unit operates autonomously, decoding each inner code individually, *layer by layer*. This still achieves an exponential suppression, albeit slower, of errors at the cost of a polynomial increase in the size of the error-correction circuit. In a FT protocol adopting this strategy, any t faults at the lower level of concatenation are correctable, hence we have the recurrence relation $t_N = (t+1)(t_{N-1}+1) - 1$, which yields

$$t_N = (t+1)^N - 1. \quad (8)$$

For a base code correcting a single error ($t=1$), we obtain the sequence $t_N = 1, 3, 7, 15, \dots$ for $d_N = 3, 9, 27, 81, \dots$. This is exponentially worse than the best case $\lfloor \frac{d^N-1}{2} \rfloor$. Nevertheless, one still has an exponential suppression of errors by increasing t_N , guaranteeing that a threshold exists [68, 69]. To understand this, we consider a circuit-level error model, where errors occur at every gate independently with probability p . Defining the logical failure rate at the N^{th} level of concatenation as p_N , with $p_0 \equiv p$, we have $p_{N+1} \sim Cp_N^{t+1}$, where $C > 1$ is a constant, corresponding to the number of combinations of $t+1$ faults leading to a logical error. Therefore, if $p < C^{-1/t}$, then recursively $p_{N+1} < p_N \forall N$, hence the suppression of the error rate is faster than the circuit growth and a threshold is attained.

To achieve the upper bound $t_N = \lfloor \frac{d^N-1}{2} \rfloor$, decoding strategies exist, but require message-passing between different layers [70]. To see how layer-by-layer decoding is not optimal, consider the concatenation of a three-bit classical repetition code with itself. This is equivalent to a nine-bit repetition code, which can correct up to four errors. However, by decoding each inner code individually, we can correct only up to three errors, as two errors in two subcodes can lead to the wrong logical state.

One can see layer-by-layer MF correction as a *decoding trade-off*: we trade fault-tolerance for lower *latency*. The latter includes: (1) *measurement latency* – the time to perform the quantum measurements; (2) *decoding latency* – the time to communicate the syndromes to the decoder, decode the syndromes, and then apply or track the corrections. Feed-forward (FF) decoding uses measurements and classical computation to achieve the t_N upper bound, but MF decoding can speed up the logical performance by allowing the decoding units to operate autonomously, addressing both measurement and decoding latencies.

Regarding the measurement latency, MF decoding is attractive for several platforms, including trapped ions and neutral atoms, as it completely side-steps the issue of having slow measurements, which is one of the main bottlenecks in a QEC round [17, 18, 23, 28–32]. In App. C we analyze the threshold measurement time for which MF decoding achieves the same fault-tolerance as a standard FF protocol, in the case of neutral-atom arrays. We estimate that the measurement latency in current state-of-the-art hardware is a significant bottleneck, such that MF schemes could outpace their conventional counterpart for small to mid-distance codes ($d \lesssim 15$).

The MF protocol avoids the decoding latency as well. The fastest decoders have been shown to operate in real-time only for small distances [8, 9]. Real-time decoding at larger distances with many logical qubits is extremely challenging, and an active field of research [71–73]. It generally requires trading tolerance for speed, too: faster decoding, such as union-find [74], has lower thresholds.

B. Circuit design

The starting point of our concatenation procedure is the MF error-correcting circuit for the 3×3 Bacon-Shor code proposed in Ref. [39]. For each subcircuit $C_X^{(n)}$ ($C_Z^{(n)}$) correcting bit-flips (phase-flips), Z-type (X -type) stabilizers are extracted to ancilla qubits, as shown in Fig. 6. Additionally, a third stabilizer $S_3 = S_1S_2$ is extracted, to be FT against circuit-level noise. For a more detailed discussion on how to choose the set of redundant stabilizers and determine the circuit’s design, we refer the reader to Ref. [39]. When concatenating this code with itself, we promote both physical qubits as well as ancilla qubits to logical qubits of the lower layer.

For the correction, we then unencode the ancilla qubits to a length- d_N repetition code using the unencoding gadgets repeatedly (see Figs. 2(d) and 2(e)), to exploit

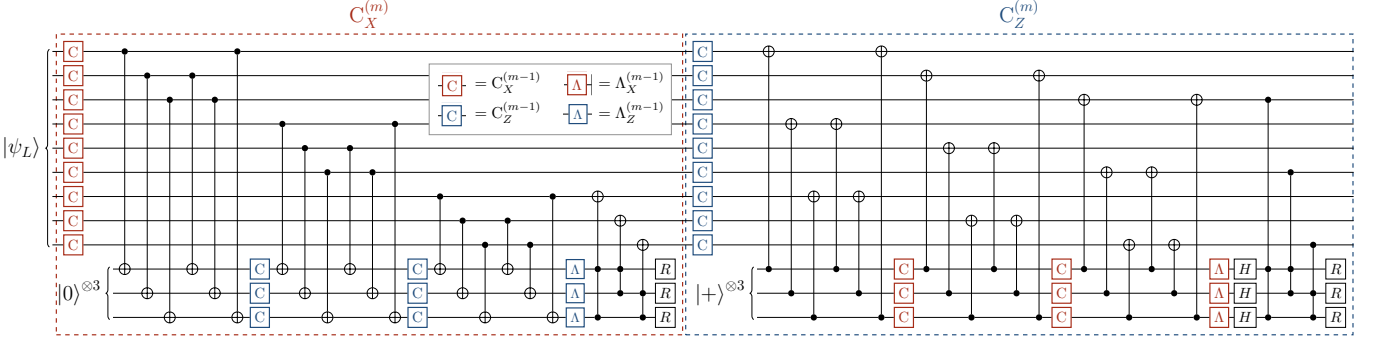


Figure 6. Measurement-free fault-tolerant QEC implementation for the concatenated Bacon-Shor code, composed of a $C_X^{(m)}$ and a $C_Z^{(m)}$ subcircuit correcting for X and Z errors, respectively, where m is the layer of concatenation. At the lowest layer $\mathcal{C}_1 \equiv \mathcal{C}$, intermediate error correcting subcircuits $C_{X/Z}^0$ and unencoding operations $\Lambda_{X/Z}^0$ are replaced by identities.

the transversality of multi-controlled gates described in Sec. II C and shown in Fig. 2(c). The unencoding protocol Λ_Z (Λ_X) is FT as all physical operations are restricted to the same column (row), thus each qubit in the resulting repetition code is independent from the others. By partially unencoding the logical ancilla qubits to a repetition code, we can then perform multi-controlled operations on the logical operations. This is why we dub this a *disposable* Toffoli gadget, since we have traded protection against certain types of errors for additional transversality. This is ideal in the MF context, as phase errors on the ancilla qubits are not influential during the correction.

Finally, when concatenating a desired code, we need to include the error-correcting rounds for the underlying layers, which we call *subbounds*. To ensure fault-tolerance, subbounds can be introduced after every single gate [75]. However, for the Bacon-Shor code we consider, we realize that in many locations this is not necessary. In particular, we can allow errors on the ancilla qubits to propagate onto the logical qubit, as long as they correspond to a gauge of the code. Therefore, we just need to place a C_Z (C_X) subbound on the ancilla qubits after having extracted a $Z_{i,j}Z_{i+1,j}$ ($X_{i,j}X_{i,j+1}$) gauge.

C. Performance

We consider the performance of the circuits presented in Sec. IV B under depolarizing noise, defined in Eq. (5). We consider the first three layers of concatenation, which correspond to $d_N = 3, 9, 27$ and respectively $t_N = 1, 3, 7$. The circuits are simulated with `stim` [76], which allows for large system-size simulations by using the stabilizer tableau formalism. To convert Toffoli-like gates into a circuit composed of Clifford gates, we note that all ancillas are reset afterwards, such that we can separately sample on their value being either 0 or 1. We therefore convert multi-qubit gates using the delayed-measurement principle

$$\begin{array}{c} \oplus \\ \parallel \end{array} \otimes \begin{array}{c} R \\ R \end{array} = \begin{array}{c} X \\ \diagup \quad \diagdown \end{array}, \quad (9)$$

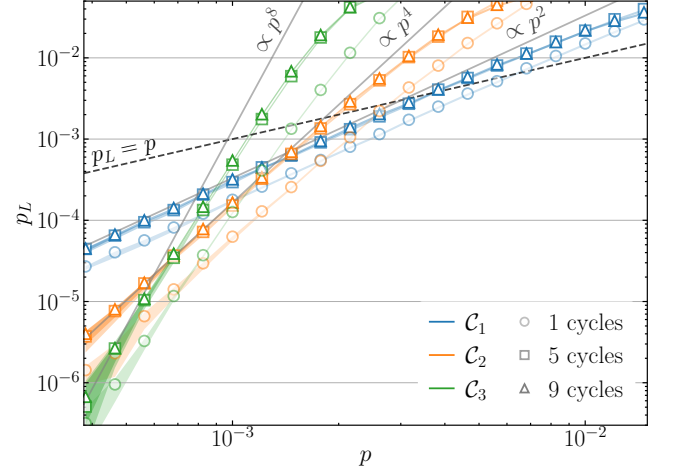


Figure 7. Logical error rate p_L versus gate error rate p , for the first three layers of concatenation. The initial state is prepared without errors, and multiple QEC rounds are performed (markers). The solid lines correspond to the asymptotic estimates, extracted from a polynomial fit.

and including the corresponding noise channels defined by Eq. (5). Classical logic in `stim` is limited to exclusive-or, so we cannot benefit from the faster compiled simulator, but we fall back to simulating the circuits using the slower tableau simulator. We can then stochastically sample noisy circuits, simulating, for each initial state, up to 2^{20} realizations or 2^{10} failures, whichever comes first.

In Fig. 7, we show the logical error rate p_L , calculated by averaging over the eigenstates of the logical Pauli operators [77]. The numerical results indicate that the failure rate of \mathcal{C}_N scales asymptotically as p^{t_N+1} , within the sampling uncertainties. This is the expected behavior for a protocol that is robust against t_N faults at the circuit level. Furthermore, for real implementations, it is worth noticing that the pseudothreshold p_* is at a level that is attainable by current state-of-the-art experiments. In particular, we extract $p_* \simeq 3.6 \times 10^{-3}$, 1.9×10^{-3} and 1.1×10^{-3} for the first three levels of concatenation. Overall, these results indicate that such MF error-correcting protocols can

achieve below-breakeven logical error rates in near-term quantum hardware, for which physical error rates below 0.1% are believed to be achievable.

V. OUTLOOK

We have constructed a fully fault-tolerant architecture for universal and scalable quantum computation that does not require any measurements. By performing a measurement-free gauge fixing and code deformation, we have demonstrated a fault-tolerant protocol for the realization of a logical CCZ gate in the Bacon-Shor code. Together with the code's fault-tolerant initialization and transversal Hadamard gate, this enables measurement-free, fault-tolerant and universal operations.

Compared to other approaches based on code concatenation [57], this approach is more resource-efficient, as it requires only two additional logical registers per logical qubit. Furthermore, considering that a CCZ gate requires a decomposition in six CNOT gates and several single-qubit rotations [78, 79], the pseudo-thresholds found here are competitive, even without the need for measurements. These ideas of gauge fixing are very powerful, as well-known error-correction concepts such as lattice surgery and code deformation have been recast as a gauge-fixing procedure [80]. It is likely that in the future such concepts can be exploited in the measurement-free context, to devise more efficient universal logical operations.

For the realization of higher-distance codes, we propose to concatenate measurement-free implementations to achieve protection against an arbitrary number of faults. Remarkably, these concatenated protocols do not require a universal gate set for any given CSS code, as we use a gadget to perform the feedback operation in a hardware-efficient way. In fact, we stress that such constructions are not unique to the Bacon-Shor code, but can be adapted to codes of the CSS family as well. In particular, we note that the disposable Toffoli gadget works as well in the $d = 3$ rotated surface code, without any adaptations. By performing numerical simulations, we find that the performance is competitive and can be considered for error-correcting experiments on near-term devices. Furthermore, it can be expected that the protocols can be further tailored to a real hardware device. For example, by exploiting biased noise, the performance of measurement-free protocols can be significantly enhanced [39]. Furthermore, neutral atoms provide an ideal platform for the implementation of such protocols, as native CCZ operations have been demonstrated [81]. In the case where such operations are not available, the protocols can be adapted without spoiling fault-tolerance. As an example, in Fig. 8, we show that correction operations can always be decomposed fault-tolerantly, by copying the control qubits to an auxiliary register, and performing a simplified decomposition of the feedback operation.

Altogether, this architecture requires non-local, but heavily parallelizable operations. This is an ideal setting

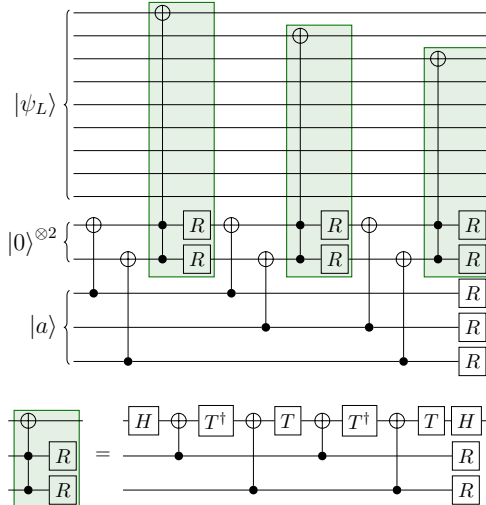


Figure 8. Decomposition of the correction step for the 3×3 Bacon-Shor code in Fig. 6 in terms of two-qubit gates. By copying the control qubits in the ancilla register $|a\rangle$, we can then use a Toffoli-reset gadget with fewer gates than the full decomposition [38].

for neutral-atom platforms, which have demonstrated parallel Clifford operations and parallel shuttling of multiple registers for the realization of transversal entangling operations [23, 24]. Furthermore, continuous loading of atoms provides a reservoir of fresh qubits, which can emulate reset operations in a scalable way [40–42]. Despite a potential performance overhead, measurement-free protocols can be a valid alternative to significantly speed up the *logical clock rate*. In App. C, we perform ‘back-of-the envelope’ calculations that suggest that for fault-tolerant experiments in the foreseeable future ($d \lesssim 15$), measurement times would need to significantly decrease to match the clock times of their measurement-free counterpart. This further motivates measurement-free error correction as a viable and scalable pathway towards fault-tolerant quantum computation.

ACKNOWLEDGMENTS

We acknowledge inspiring discussions with Gavin Brennen and Johannes Zeiher. AP acknowledges partial funding from the Defense Advanced Research Projects Agency [under the Quantum Benchmarking (QB) program under award no. HR00112230006 and HR001121S0026 contracts], and was supported by the QuantERA grant EQUIP through the Academy of Finland, decision number 352188. The views, opinions and/or findings expressed are those of the author(s) and should not be interpreted as representing the official views or policies of the Department of Defense or the U.S. Government.

Appendix A: Transversality of controlled-gates between repetition codes and CSS codes

In this appendix, we show that a logical $C^k X$ ($C^k Z$) gate on a distance- d CSS code can be controlled from k length- d bit-flip repetition codes, without affecting the stabilizer structure of the logical qubits involved. These consist of d physical $C^k X$ ($C^k Z$) gates targeting the d qubits of the code supporting the X_L (Z_L) operator.

For the CX gate, using the well known propagation rules

$$\begin{array}{l} \text{---} \boxed{X} \text{---} = \text{---} \bullet \boxed{X} \text{---}, \quad \text{---} \boxed{X} \oplus \text{---} = \text{---} \bullet \oplus \boxed{X} \text{---}, \\ \text{---} \boxed{Z} \text{---} = \text{---} \bullet \boxed{Z} \text{---}, \quad \text{---} \boxed{Z} \oplus \text{---} = \text{---} \bullet \oplus \boxed{Z} \text{---}, \end{array} \quad (\text{A1})$$

we realize that the only non-trivial propagation are the S^Z stabilizers of the code overlapping with X_L , which get mapped to the stabilizers of the repetition code. By definition, X_L commutes with the stabilizers, meaning every overlap with S^Z stabilizers involves an even number of qubits. But an even product of distinct Z operators can always be absorbed by the stabilizer generators of the repetition code. In the case of a CZ gate, the targets support the Z_L operator, and equivalent results are obtained by using the identity $CZ = (I \otimes H)CX(I \otimes H)$. By symmetry these arguments also hold for unidirectional gates on length d phase-flip repetition codes controlled by distance- d CSS codes.

We can now extend these result to three-qubit gates as well. Again, using the propagation rules for the Toffoli gate

$$\begin{array}{l} \text{---} \boxed{X} \text{---} = \text{---} \bullet \boxed{X} \text{---}, \quad \text{---} \bullet \text{---} = \text{---} \bullet \text{---}, \\ \text{---} \boxed{Z} \text{---} = \text{---} \bullet \boxed{Z} \text{---}, \quad \text{---} \boxed{Z} \text{---} = \text{---} \bullet \boxed{Z} \text{---}, \end{array} \quad (\text{A2})$$

the only non-trivial propagation arises from the S^Z stabilizers of the code overlapping with X_L . The even number of overlapping qubits results in an even number of CZ operations between the controlling bit-flip codes, which reciprocally cancel. Similarly, in the CCZ gate, the non-trivial propagation is due the intersection of S^X stabilizers and Z_L , which again results in the propagation of an even number of CZ s, which reciprocally cancel out.

In general, the $C^k X$ ($C^k Z$) gates controlled on the bit-flip codes only have non-trivial propagation of the S^Z (S^X) stabilizers of the code overlapping with X_L (Z_L). These lead to an even number of $C^{k-1}Z$ gates between the controlling bit-flip codes, which mutually cancel out, thus preserving the stabilizer structure.

Appendix B: Steane-type MF gauge fixing

As an alternative, we also propose a gauge fixing inspired by Steane-type MF QEC [38, 43], which both corrects single-qubit bit-flips and enforces the Shor gauge, using fewer qubits if fast resets are available.

This protocol is illustrated in Fig. 9. The main idea is to treat each row one at a time, extracting each ZZ gauge operator to detect bit-flips (orange box). For each bit flip, we apply a XX gauge operator between the current row (green box) and the next one (purple box). This sets each of the Z -gauges to their $+1$ eigenvalue, and moves single bit-flip errors to the last row. We can then perform a similar bit-flip correction on the last row to correct for a potentially remaining bit-flip. As with Steane-type QEC, this scheme avoids the propagation of more than one error.

The scheme can be sped up, by extracting ZZ gauge operators of the top and bottom rows simultaneously, and then applying the XX gauge operator between said row and, respectively, the one below or above. By repeating this process iteratively, between rows progressively closer to the middle, errors are moved to the middle row. Finally, one round of extraction and correction on the middle row corrects a potentially remaining bit-flip.

A comparison of the two different gauge fixing protocols presented is shown in Fig. 10. We note that the performance of the teleportation circuit is independent of the initial state's gauge, while the Steane-type gauge fixing has a higher error rate when the gauge is incorrect.

Appendix C: Practical considerations

In this section, we compare the implementation of the MF protocols and more conventional QEC protocols on a potential neutral-atom platform, from the point of view of logical clock time. In particular, we assume a two-dimensional array of atoms, with parallel shuttling capabilities. Since the concatenation procedure increases the footprint of the logical register, it is important to account for potentially long shuttling times. For measurements, we consider the situation of either reconfigurable arrays with a separate readout zone [23], or a static array with local imaging of ancillae, enabled for example by shelving of the data qubits to different atomic levels.

For a MF QEC protocol, such as the one presented in Fig. 7, the total time required for a subcircuit C^N at N levels of concatenation can be broken down as

$$T_C^{(N)} = T_{\text{SE}}^{(N)} + T_{\text{FB}}^{(N)}, \quad (\text{C1})$$

where $T_{\text{SE}}^{(N)}$ is the time required for a syndrome extraction and $T_{\text{FB}}^{(N)}$ that of a feedback operation. For simplicity, we only consider shuttling and measurement times, since these are typically much more important than the execution time of individual gates [23, 82]. We denote the time required to shuttle a lattice spacing as $\delta\tau$.

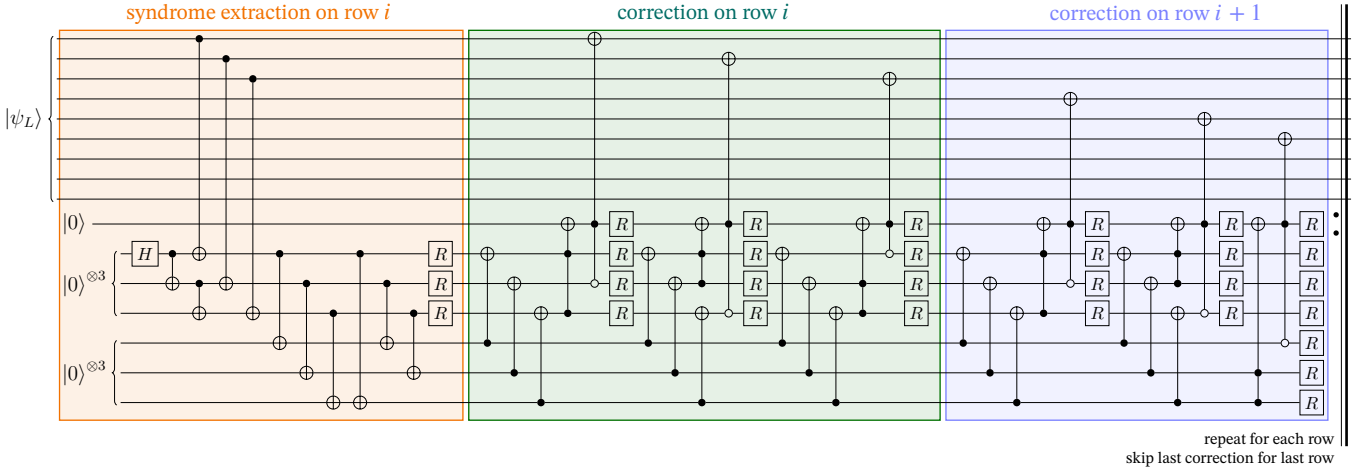


Figure 9. Gauge fixing by adapting Steane-type error correction. This circuit maps the X errors of a single row into a three-qubit cat state, decodes it by a redundant extraction of the parities [39] (orange box), and, if a bit flip occurred, applies a XX gauge operator between the current row (green box) and the next one (purple box). This circuit is repeated for all rows except for the last one, where remaining bit-flip errors are extracted and then corrected by applying only the first part of the corrections.

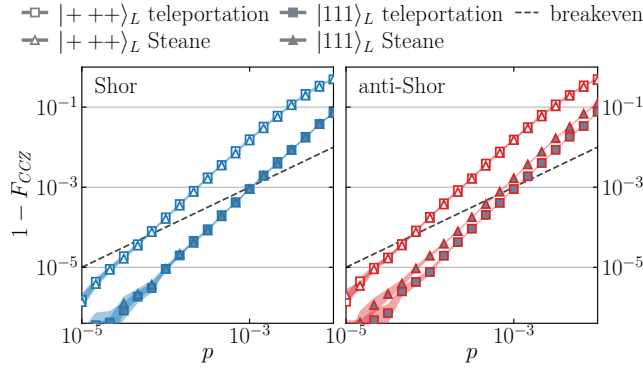


Figure 10. Logical error rate of the two gauge-fixing protocols, starting from the two initial states considered in Fig. 5, in either the Shor (left) or anti-Shor gauge (right).

We now consider the individual contributions to Eq. (C1). We assume the parallel extraction of individual stabilizers, which corresponds to a time $T_{\text{SE}}^{(N)} \sim \kappa d_N \delta\tau + 4T_{\text{C}}^{(N-1)}$. This is applicable to the Bacon-Shor code, since we can devise an alternative MF QEC protocol using four ancilla qubits instead of three, cf. Fig. 11. The advantage of this protocol is that it avoids measuring the stabilizer S_3 (cf. Sec. IV B), which requires longer-range interactions, by measuring S_1 and S_2 twice. Compared to Fig. 1(e), it exhibits a slightly lower pseudothreshold, despite having more redundancy. In particular, for this protocol $\kappa = 2(1 + \sqrt{2})$, as shown in Fig. 11. The shuttling schedule presented is compatible with the constraints imposed by the acousto-optical-deflectors (AODs) used to steer atoms in neutral-atom hardware [83, 84]. For the feedback operation, we require two movements of length d_{N-1} for the unencoding and two movements

of length d_N for the application of the Toffoli gates, i.e. $T_{\text{FB}}^{(N)} = 2d_N \delta\tau + 2d_{N-1} \delta\tau = (2d + 2)d_{N-1} \delta\tau$.

Plugging these results in Eq. (C1), we obtain, for $d = 3$, $T_{\text{C}}^{(N)} = 4T_{\text{C}}^{(N-1)} + (3\kappa + 8)d_{N-1} \delta\tau$, yielding [85]

$$T_{\text{C}}^{(N)} = (3\kappa + 8)\delta\tau \sum_{n=1}^N 4^{n-1} 3^{N-n} = (3\kappa + 8)(4^N - 3^N)\delta\tau. \quad (\text{C2})$$

For comparing with equivalent feed-forward (FF) implementations, we use a code that is equivalent by the number of correctable errors t_N rather than the distance, cf. Eq. (8). It is then helpful to write the total time in terms of it, which, as $t_N + 1 = 2^N$, reads

$$T_{\text{C}}^{(N)} = (3\kappa + 8) \left[2^N - \left(\frac{3}{2} \right)^N \right] (t_N + 1)\delta\tau. \quad (\text{C3})$$

For the FF implementation, we consider a logical qubit encoded in a $d \times d$ register, using some CSS code such as the rotated surface code, allowing for local stabilizer extractions without shuttling. We assume that by correctly decoding the syndrome information, we can correct up to $t = \lfloor \frac{d-1}{2} \rfloor$ faults on the data qubits.

In this setting, a QEC cycle is then dominated by the measurement time T_M . In particular, for an extraction of a single type of syndromes, the measurements of the stabilizers is generally performed d times to be robust against circuit-level noise. Within this measurement time we can also include the shuttling time to a separate readout zone, which can be non-negligible [23].

The breakeven measurement time T_M^* , for which the MF protocol with shuttling would match the FF implementation, for the same t , is then

$$T_M^* = \frac{t_N + 1}{2t_N + 1} (3\kappa + 8) \left[2^N - \left(\frac{3}{2} \right)^N \right] \delta\tau. \quad (\text{C4})$$

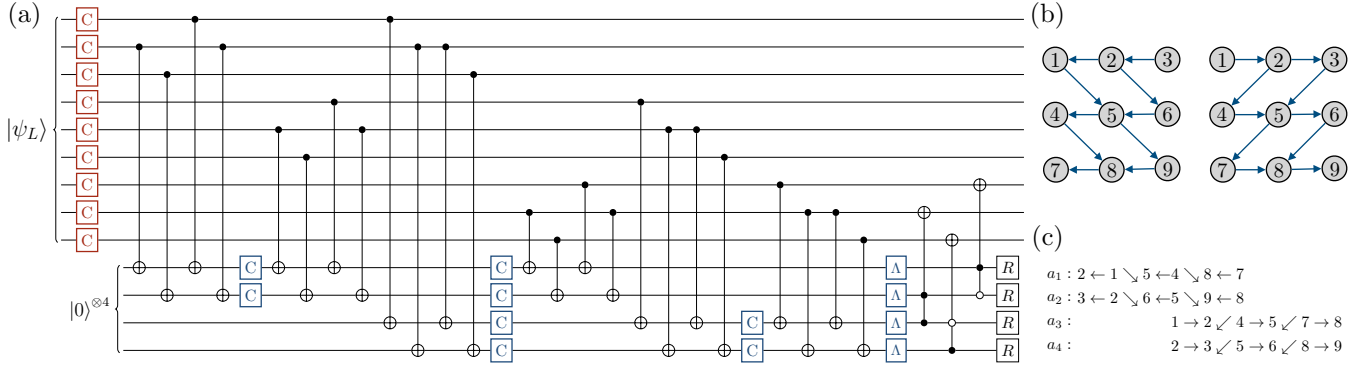


Figure 11. (a) Alternative measurement-free and fault-tolerant QEC implementation for the Bacon-Shor code, using four ancillae. The colored operations follow the same convention of Fig. 6, indicating subcircuit error correction and unencoding routines. (b) Shuttling pattern for the first two (left) and last two (right) ancillae. (c) Shuttling schedule for the syndrome extraction, showing which data qubit each ancilla a_i interacts with at a certain moment in time, and the direction of the shuttling in between. The order with which ancillae interact with data qubits is important to preserve fault-tolerance [39]. The schedule proposed is chosen to maximize the number of parallel operations, while also avoiding the propagation of uncorrectable errors from the ancillae to the data qubits.

With a conservative estimate of $\delta\tau = 10 \mu\text{s}$ [82], we obtain $T_M^* \simeq 0.08 \text{ ms}$, 0.22 ms and 0.55 ms for $N = 1$, 2 and 3 . Current state-of-the-art experiments across various atomic species and qubit encodings have attained a T_M that range between 1 ms to 20 ms [23, 29–32, 86, 87], highlighting the competitiveness of our MF approach.

On the one hand, the FF implementation could be improved in principle by not applying d rounds of syndrome extraction for every type of stabilizer, as recent research has shown that for a logical computation fewer rounds of measurements can be performed and fault-tolerance

can still be preserved, at the price of a more complicated decoding [88]. It remains to be seen if such approaches can be adapted to the measurement-free setting as well. On the other hand, for a FF implementation of a logical computation it is important to take into account shuttling times to a readout zone. For a $L \times L$ patch of logical registers, the measurement time then has an additional shuttling time overhead of $dL\delta\tau$. Considering that practically-relevant quantum algorithms will require hundreds to thousands logical qubits [89], future experiments will need to tackle such increasing overhead.

-
- [1] B. M. Terhal, Quantum error correction for quantum memories, *Rev. Mod. Phys.* **87**, 307 (2015).
- [2] E. T. Campbell, B. M. Terhal, and C. Vuillot, Roads towards fault-tolerant universal quantum computation, *Nature* **549**, 172 (2017).
- [3] Google Quantum AI, Exponential suppression of bit or phase errors with cyclic error correction, *Nature* **595**, 383 (2021).
- [4] S. Krinner, N. Lacroix, A. Remm, A. Di Paolo, E. Genois, C. Leroux, C. Hellings, S. Lazar, F. Swiadek, J. Hermann, G. J. Norris, C. K. Andersen, M. Müller, A. Blais, C. Eichler, and A. Wallraff, Realizing repeated quantum error correction in a distance-three surface code, *Nature* **605**, 669 (2022).
- [5] Y. Zhao, Y. Ye, H.-L. Huang, Y. Zhang, D. Wu, H. Guan, Q. Zhu, Z. Wei, T. He, S. Cao, F. Chen, T.-H. Chung, H. Deng, D. Fan, M. Gong, C. Guo, S. Guo, L. Han, N. Li, S. Li, *et al.*, Realization of an error-correcting surface code with superconducting qubits, *Phys. Rev. Lett.* **129**, 030501 (2022).
- [6] Google Quantum AI, Suppressing quantum errors by scaling a surface code logical qubit, *Nature* **614**, 676 (2023).
- [7] R. S. Gupta, N. Sundaresan, T. Alexander, C. J. Wood, S. T. Merkel, M. B. Healy, M. Hillenbrand, T. Jochym-
- O'Connor, J. R. Wootton, T. J. Yoder, A. W. Cross, M. Takita, and B. J. Brown, Encoding a magic state with beyond break-even fidelity, *Nature* **625**, 259 (2024).
- [8] L. Caune, L. Skoric, N. S. Blunt, A. Ruban, J. McDaniel, J. A. Valery, A. D. Patterson, A. V. Gramolin, J. Mäjaniemi, K. M. Barnes, T. Bialas, O. Buğdaycı, O. Crawford, G. P. Gehér, H. Krovi, E. Matekole, C. Topal, S. Poletto, M. Bryant, K. Snyder, *et al.*, Demonstrating real-time and low-latency quantum error correction with superconducting qubits (2024), [arXiv:2410.05202](#).
- [9] Google Quantum AI and Collaborators, Quantum error correction below the surface code threshold, *Nature* [10.1038/s41586-024-08449-y](#) (2024).
- [10] Google Quantum AI and Collaborators, Demonstrating dynamic surface codes (2024), [arXiv:2412.14360](#).
- [11] N. Lacroix, A. Bourassa, F. J. H. Heras, L. M. Zhang, J. Bausch, A. W. Senior, T. Edlich, N. Shutty, V. Sivak, A. Bengtsson, M. McEwen, O. Higgott, D. Kafri, J. Claes, A. Morvan, Z. Chen, A. Zalcman, S. Madhuk, R. Acharya, L. A. Beni, *et al.*, Scaling and logic in the color code on a superconducting quantum processor (2024), [arXiv:2412.14256](#).
- [12] L. Egan, D. M. Debroy, C. Noel, A. Risinger, D. Zhu, D. Biswas, M. Newman, M. Li, K. R. Brown, M. Cetina,

- and C. Monroe, Fault-tolerant control of an error-corrected qubit, *Nature* **598**, 281 (2021).
- [13] C. Ryan-Anderson, J. G. Bohnet, K. Lee, D. Gresh, A. Hankin, J. P. Gaebler, D. Francois, A. Chernoguzov, D. Lucchetti, N. C. Brown, T. M. Gatterman, S. K. Halit, K. Gilmore, J. A. Gerber, B. Neyenhuis, D. Hayes, and R. P. Stutz, Realization of real-time fault-tolerant quantum error correction, *Phys. Rev. X* **11**, 041058 (2021).
- [14] J. Hilder, D. Pijn, O. Onishchenko, A. Stahl, M. Orth, B. Lekitsch, A. Rodriguez-Blanco, M. Müller, F. Schmidt-Kaler, and U. G. Poschinger, Fault-tolerant parity readout on a shuttling-based trapped-ion quantum computer, *Phys. Rev. X* **12**, 011032 (2022).
- [15] L. Postler, S. Heußen, I. Pogorelov, M. Rispler, T. Feldker, M. Meth, C. D. Marciniak, R. Stricker, M. Ringbauer, R. Blatt, P. Schindler, M. Müller, and T. Monz, Demonstration of fault-tolerant universal quantum gate operations, *Nature* **605**, 675 (2022).
- [16] Y. Wang, S. Simsek, T. M. Gatterman, J. A. Gerber, K. Gilmore, D. Gresh, N. Hewitt, C. V. Horst, M. Matheny, T. Mengle, B. Neyenhuis, and B. Criger, Fault-tolerant one-bit addition with the smallest interesting color code, *Sci. Adv.* **10**, eado9024 (2024).
- [17] L. Postler, F. Butt, I. Pogorelov, C. D. Marciniak, S. Heußen, R. Blatt, P. Schindler, M. Rispler, M. Müller, and T. Monz, Demonstration of fault-tolerant Steane quantum error correction, *PRX Quantum* **5**, 030326 (2024).
- [18] I. Pogorelov, F. Butt, L. Postler, C. D. Marciniak, P. Schindler, M. Müller, and T. Monz, Experimental fault-tolerant code switching (2024), [arXiv:2403.13732](#).
- [19] C. Ryan-Anderson, N. C. Brown, C. H. Baldwin, J. M. Dreiling, C. Foltz, J. P. Gaebler, T. M. Gatterman, N. Hewitt, C. Holliman, C. V. Horst, J. Johansen, D. Lucchetti, T. Mengle, M. Matheny, Y. Matsuoka, K. Mayer, M. Mills, S. A. Moses, B. Neyenhuis, J. Pino, *et al.*, High-fidelity teleportation of a logical qubit using transversal gates and lattice surgery, *Science* **385**, 1327 (2024).
- [20] M. P. da Silva, C. Ryan-Anderson, J. M. Bello-Rivas, A. Chernoguzov, J. M. Dreiling, C. Foltz, F. Frachon, J. P. Gaebler, T. M. Gatterman, L. Grans-Samuelsson, D. Hayes, N. Hewitt, J. Johansen, D. Lucchetti, M. Mills, S. A. Moses, B. Neyenhuis, A. Paz, J. Pino, P. Siegfried, *et al.*, Demonstration of logical qubits and repeated error correction with better-than-physical error rates (2024), [arXiv:2404.02280](#).
- [21] N. Berthelsen, J. Dreiling, C. Foltz, J. P. Gaebler, T. M. Gatterman, D. Gresh, N. Hewitt, M. Mills, S. A. Moses, B. Neyenhuis, P. Siegfried, and D. Hayes, Experiments with the 4d surface code on a qcd quantum computer (2024), [arXiv:2408.08865](#).
- [22] M. H. Abobeih, Y. Wang, J. Randall, S. J. H. Loenen, C. E. Bradley, M. Markham, D. J. Twitchen, B. M. Terhal, and T. H. Taminiau, Fault-tolerant operation of a logical qubit in a diamond quantum processor, *Nature* **606**, 884 (2022).
- [23] D. Bluvstein, S. J. Evered, A. A. Geim, S. H. Li, H. Zhou, T. Manovitz, S. Ebadi, M. Cain, M. Kalinowski, D. Hangleiter, J. P. Bonilla Ataides, N. Maskara, I. Cong, X. Gao, P. Sales Rodriguez, T. Karolyshyn, G. Semeghini, M. J. Gullans, M. Greiner, V. Vuletić, *et al.*, Logical quantum processor based on reconfigurable atom arrays, *Nature* **626**, 58 (2024).
- [24] B. W. Reichardt, A. Paetznick, D. Aasen, I. Basov, J. M. Bello-Rivas, P. Bonderson, R. Chao, W. van Dam, M. B. Hastings, A. Paz, M. P. da Silva, A. Sundaram, K. M. Svore, A. Vaschillo, Z. Wang, M. Zanner, W. B. Cairncross, C.-A. Chen, D. Crow, H. Kim, *et al.*, Logical computation demonstrated with a neutral atom quantum processor (2024), [arXiv:2411.11822](#).
- [25] M. J. Bedalov, M. Blakely, P. D. Buttler, C. Carnahan, F. T. Chong, W. C. Chung, D. C. Cole, P. Goiporia, P. Gokhale, B. Heim, G. T. Hickman, E. B. Jones, R. A. Jones, P. Khalate, J.-S. Kim, K. W. Kuper, M. T. Lichtman, S. Lee, D. Mason, N. A. Neff-Mallon, *et al.*, Fault-tolerant operation and materials science with neutral atom logical qubits (2024), [arXiv:2412.07670](#).
- [26] P. S. Rodriguez, J. M. Robinson, P. N. Jepsen, Z. He, C. Duckering, C. Zhao, K.-H. Wu, J. Campo, K. Baggett, M. Kwon, T. Karolyshyn, P. Weinberg, M. Cain, S. J. Evered, A. A. Geim, M. Kalinowski, S. H. Li, T. Manovitz, J. Amato-Grill, J. I. Basham, *et al.*, Experimental demonstration of logical magic state distillation (2024), [arXiv:2412.15165](#).
- [27] D. Gottesman, *Stabilizer codes and quantum error correction*, Ph.D. thesis, California Institute of Technology (1997).
- [28] T. M. Graham, L. Phuttitarn, R. Chinnarasu, Y. Song, C. Poole, K. Jooya, J. Scott, A. Scott, P. Eichler, and M. Saffman, Midcircuit measurements on a single-species neutral alkali atom quantum processor, *Phys. Rev. X* **13**, 041051 (2023).
- [29] K. Singh, C. E. Bradley, S. Anand, V. Ramesh, R. White, and H. Bernien, Mid-circuit correction of correlated phase errors using an array of spectator qubits, *Science* **380**, 1265 (2023).
- [30] W. Huie, L. Li, N. Chen, X. Hu, Z. Jia, W. K. C. Sun, and J. P. Covey, Repetitive readout and real-time control of nuclear spin qubits in ^{171}Yb atoms, *PRX Quantum* **4**, 030337 (2023).
- [31] J. W. Lis, A. Senoo, W. F. McGrew, F. Rönchen, A. Jenkins, and A. M. Kaufman, Midcircuit operations using the exitomg architecture in neutral atom arrays, *Phys. Rev. X* **13**, 041035 (2023).
- [32] M. A. Norcia, W. B. Cairncross, K. Barnes, P. Battaglino, A. Brown, M. O. Brown, K. Cassella, C.-A. Chen, R. Coxe, D. Crow, J. Epstein, C. Griger, A. M. W. Jones, H. Kim, J. M. Kindem, J. King, S. S. Kondov, K. Kotru, J. Lauigan, M. Li, *et al.*, Midcircuit qubit measurement and rearrangement in a ^{171}Yb atomic array, *Phys. Rev. X* **13**, 041034 (2023).
- [33] G. A. Paz-Silva, G. K. Brennen, and J. Twamley, Fault tolerance with noisy and slow measurements and preparation, *Phys. Rev. Lett.* **105**, 100501 (2010).
- [34] C.-K. Li, M. Nakahara, Y.-T. Poon, N.-S. Sze, and H. Tomita, Recovery in quantum error correction for general noise without measurement, *Quantum Inf. Comput.* **12**, 149 (2012).
- [35] D. Crow, R. Joynt, and M. Saffman, Improved error thresholds for measurement-free error correction, *Phys. Rev. Lett.* **117**, 130503 (2016).
- [36] H. E. Ercan, J. Ghosh, D. Crow, V. N. Premakumar, R. Joynt, M. Friesen, and S. N. Coppersmith, Measurement-free implementations of small-scale surface codes for quantum-dot qubits, *Phys. Rev. A* **97**, 012318 (2018).
- [37] M. A. Perlin, V. N. Premakumar, J. Wang, M. Saffman, and R. Joynt, Fault-tolerant measurement-free quantum

- error correction with multiqubit gates, *Phys. Rev. A* **108**, 062426 (2023).
- [38] S. Heußen, D. F. Locher, and M. Müller, Measurement-free fault-tolerant quantum error correction in near-term devices, *PRX Quantum* **5**, 010333 (2024).
- [39] S. Veroni, M. Müller, and G. Giudice, Optimized measurement-free and fault-tolerant quantum error correction for neutral atoms, *Phys. Rev. Res.* **6**, 043253 (2024).
- [40] K. Singh, S. Anand, A. Pocklington, J. T. Kemp, and H. Bernien, Dual-element, two-dimensional atom array with continuous-mode operation, *Phys. Rev. X* **12**, 011040 (2022).
- [41] M. A. Norcia, H. Kim, W. B. Cairncross, M. Stone, A. Ryou, M. Jaffe, M. O. Brown, K. Barnes, P. Battaglino, T. C. Bohdanowicz, A. Brown, K. Cassella, C.-A. Chen, R. Coxe, D. Crow, J. Epstein, C. Griger, E. Halperin, F. Hummel, A. M. W. Jones, *et al.*, Iterative assembly of ^{171}Yb atom arrays with cavity-enhanced optical lattices, *PRX Quantum* **5**, 030316 (2024).
- [42] F. Gyger, M. Ammenwerth, R. Tao, H. Timme, S. Snigirev, I. Bloch, and J. Zeiher, Continuous operation of large-scale atom arrays in optical lattices, *Phys. Rev. Res.* **6**, 033104 (2024).
- [43] A. M. Steane, Active stabilization, quantum computation, and quantum state synthesis, *Phys. Rev. Lett.* **78**, 2252 (1997).
- [44] B. Eastin and E. Knill, Restrictions on transversal encoded quantum gate sets, *Phys. Rev. Lett.* **102**, 110502 (2009).
- [45] S. Bravyi and R. König, Classification of topologically protected gates for local stabilizer codes, *Phys. Rev. Lett.* **110**, 170503 (2013).
- [46] S. Bravyi and A. Kitaev, Universal quantum computation with ideal clifford gates and noisy ancillas, *Phys. Rev. A* **71**, 022316 (2005).
- [47] E. T. Campbell, H. Anwar, and D. E. Browne, Magic-state distillation in all prime dimensions using quantum reed-muller codes, *Phys. Rev. X* **2**, 041021 (2012).
- [48] E. T. Campbell and M. Howard, Unified framework for magic state distillation and multiqubit gate synthesis with reduced resource cost, *Phys. Rev. A* **95**, 022316 (2017).
- [49] J. O’Gorman and E. T. Campbell, Quantum computation with realistic magic-state factories, *Phys. Rev. A* **95**, 032338 (2017).
- [50] D. Litinski, Magic State Distillation: Not as Costly as You Think, *Quantum* **3**, 205 (2019).
- [51] J. T. Anderson, G. Duclos-Cianci, and D. Poulin, Fault-tolerant conversion between the Steane and reed-muller quantum codes, *Phys. Rev. Lett.* **113**, 080501 (2014).
- [52] M. E. Beverland, A. Kubica, and K. M. Svore, Cost of universality: A comparative study of the overhead of state distillation and code switching with color codes, *PRX Quantum* **2**, 020341 (2021).
- [53] F. Butt, S. Heußen, M. Rispler, and M. Müller, Fault-tolerant code-switching protocols for near-term quantum processors, *PRX Quantum* **5**, 020345 (2024).
- [54] T. J. Yoder, Universal fault-tolerant quantum computation with Bacon-Shor codes (2017), [arXiv:1705.01686](https://arxiv.org/abs/1705.01686).
- [55] T. J. Yoder, R. Takagi, and I. L. Chuang, Universal fault-tolerant gates on concatenated stabilizer codes, *Phys. Rev. X* **6**, 031039 (2016).
- [56] A. Paetznick and B. W. Reichardt, Universal fault-tolerant quantum computation with only transversal gates and error correction, *Phys. Rev. Lett.* **111**, 090505 (2013).
- [57] T. Jochym-O’Connor and R. Laflamme, Using concatenated quantum codes for universal fault-tolerant quantum gates, *Phys. Rev. Lett.* **112**, 010505 (2014).
- [58] C. Chamberland, T. Jochym-O’Connor, and R. Laflamme, Overhead analysis of universal concatenated quantum codes, *Phys. Rev. A* **95**, 022313 (2017).
- [59] F. Butt, D. F. Locher, K. Brechtelsbauer, H. P. Büchler, and M. Müller, Measurement-free, scalable and fault-tolerant universal quantum computing (2024), [arXiv:2410.13568](https://arxiv.org/abs/2410.13568).
- [60] A. R. Calderbank and P. W. Shor, Good quantum error-correcting codes exist, *Phys. Rev. A* **54**, 1098 (1996).
- [61] A. M. Steane, Error correcting codes in quantum theory, *Phys. Rev. Lett.* **77**, 793 (1996).
- [62] D. Bacon, Operator quantum error-correcting subsystems for self-correcting quantum memories, *Phys. Rev. A* **73**, 012340 (2006).
- [63] P. Aliferis and A. W. Cross, Subsystem fault tolerance with the Bacon-Shor code, *Phys. Rev. Lett.* **98**, 220502 (2007).
- [64] P. W. Shor, Scheme for reducing decoherence in quantum computer memory, *Phys. Rev. A* **52**, R2493 (1995).
- [65] M. Li, D. Miller, M. Newman, Y. Wu, and K. R. Brown, 2d compass codes, *Phys. Rev. X* **9**, 021041 (2019).
- [66] `SparseStates.jl`, GitHub repository.
- [67] S. Jaques and T. Häner, Leveraging state sparsity for more efficient quantum simulations, *ACM Trans. Quantum Comput.* **3**, 10.1145/3491248 (2022).
- [68] E. Knill, R. Laflamme, and W. H. Zurek, Resilient quantum computation, *Science* **279**, 342 (1998).
- [69] D. Aharonov and M. Ben-Or, Fault-tolerant quantum computation with constant error rate, *SIAM Journal on Computing* **38**, 1207 (2008).
- [70] D. Poulin, Optimal and efficient decoding of concatenated quantum block codes, *Phys. Rev. A* **74**, 052333 (2006).
- [71] F. Battistel, C. Chamberland, K. Johar, R. W. J. Overwater, F. Sebastian, L. Skoric, Y. Ueno, and M. Usman, Real-time decoding for fault-tolerant quantum computing: progress, challenges and outlook, *Nano Futures* **7**, 10.1088/2399-1984/aceba6 (2023).
- [72] L. Skoric, D. E. Browne, K. M. Barnes, N. I. Gillespie, and E. T. Campbell, Parallel window decoding enables scalable fault tolerant quantum computation, *Nat. Commun.* **14**, 10.1038/s41467-023-42482-1 (2023).
- [73] N. Liyanage, Y. Wu, S. Tagare, and L. Zhong, Fpga-based distributed union-find decoder for surface codes, *IEEE Trans. Quantum Eng.* **5**, 10.1109/tqe.2024.3467271 (2024).
- [74] N. Delfosse and N. H. Nickerson, Almost-linear time decoding algorithm for topological codes, *Quantum* **5**, 595 (2021).
- [75] P. Aliferis, D. Gottesman, and J. Preskill, Quantum accuracy threshold for concatenated distance-3 codes (2005), [arXiv:quant-ph/0504218](https://arxiv.org/abs/quant-ph/0504218).
- [76] C. Gidney, Stim: a fast stabilizer circuit simulator, *Quantum* **5**, 497 (2021).
- [77] L. H. Pedersen, N. M. Møller, and K. Mølmer, Fidelity of quantum operations, *Physics Letters A* **367**, 47 (2007).
- [78] M. A. Nielsen and I. L. Chuang, *Quantum Computation and Quantum Information: 10th Anniversary Edition* (Cambridge University Press, Cambridge, 2010).
- [79] V. V. Shende and I. L. Markov, On the cnot-cost of toffoli gates, *Quantum Inf. Comput.* **9**, 461 (2008).
- [80] C. Vuillot, L. Lao, B. Criger, C. García Almudéver, K. Ber-

- tels, and B. M. Terhal, Code deformation and lattice surgery are gauge fixing, *New Journal of Physics* **21**, 033028 (2019).
- [81] S. J. Evered, D. Bluvstein, M. Kalinowski, S. Ebadi, T. Manovitz, H. Zhou, S. H. Li, A. A. Geim, T. T. Wang, N. Maskara, H. Levine, G. Semeghini, M. Greiner, V. Vuletić, and M. D. Lukin, High-fidelity parallel entangling gates on a neutral-atom quantum computer, *Nature* **622**, 268 (2023).
- [82] D. Bluvstein, H. Levine, G. Semeghini, T. T. Wang, S. Ebadi, M. Kalinowski, A. Keesling, N. Maskara, H. Pichler, M. Greiner, V. Vuletić, and M. D. Lukin, A quantum processor based on coherent transport of entangled atom arrays, *Nature* **604**, 451 (2022).
- [83] L. Schmid, D. F. Locher, M. Rispler, S. Blatt, J. Zeiher, M. Müller, and R. Wille, Computational capabilities and compiler development for neutral atom quantum processors—connecting tool developers and hardware experts, *Quantum Science and Technology* **9**, 10.1088/2058-9565/ad33ac (2024).
- [84] N. Constantinides, A. Fahimniya, D. Devulapalli, D. Bluvstein, M. J. Gullans, J. V. Porto, A. M. Childs, and A. V. Gorshkov, Optimal routing protocols for reconfigurable atom arrays (2024), [arXiv:2411.05061](https://arxiv.org/abs/2411.05061).
- [85] This equation slightly overestimates the time, as it incorrectly assumes the use of an unencoding gadget also at the lowest level of concatenation. However, this slight difference is negligible for the purposes of our heuristic calculations.
- [86] R. Finkelstein, R. B.-S. Tsai, X. Sun, P. Scholl, S. Direkci, T. Gefen, J. Choi, A. L. Shaw, and M. Endres, Universal quantum operations and ancilla-based read-out for tweezer clocks, *Nature* **634**, 321 (2024).
- [87] A. G. Radnaev, W. C. Chung, D. C. Cole, D. Mason, T. G. Ballance, M. J. Bedalov, D. A. Belknap, M. R. Berman, M. Blakely, I. L. Bloomfield, P. D. Buttler, C. Campbell, A. Chopinaud, E. Copenhaver, M. K. Dawes, S. Y. Eu-banks, A. J. Friss, D. M. Garcia, J. Gilbert, M. Gillette, *et al.*, A universal neutral-atom quantum computer with individual optical addressing and non-destructive readout (2024), [arXiv:2408.08288](https://arxiv.org/abs/2408.08288).
- [88] H. Zhou, C. Zhao, M. Cain, D. Bluvstein, C. Duckering, H.-Y. Hu, S.-T. Wang, A. Kubica, and M. D. Lukin, Algorithmic fault tolerance for fast quantum computing (2024), [arXiv:2406.17653](https://arxiv.org/abs/2406.17653).
- [89] A. M. Dalzell, S. McArdle, M. Berta, P. Bienias, C.-F. Chen, A. Gilyén, C. T. Hann, M. J. Kastoryano, E. T. Khabiboulline, A. Kubica, G. Salton, S. Wang, and F. G. S. L. Brandão, Quantum algorithms: A survey of applications and end-to-end complexities (2023), [arXiv:2310.03011](https://arxiv.org/abs/2310.03011).